

RESEARCH ARTICLE | JANUARY 27 2025

Transmission of photonic entangled states encoded via eigenstates of photon-number parity operator

Liang Bin ; Dong-Xuan Zhang ; Lei Chen; Yi-Hao Kang ; Zhi-Rong Zhong ; Qi-Ping Su ; Chui-Ping Yang 



Appl. Phys. Lett. 126, 044001 (2025)
<https://doi.org/10.1063/5.0249115>



Articles You May Be Interested In

Realization of dark state in a three-dimensional transmon superconducting qutrit

Appl. Phys. Lett. (November 2015)

Development of some two and three qutrit quantum logic gates

AIP Conf. Proc. (November 2019)

Preparation of hybrid *W* entangled states between superconducting qubits and microwave resonators in circuit QED

Appl. Phys. Lett. (October 2024)

Transmission of photonic entangled states encoded via eigenstates of photon-number parity operator

EP

Cite as: Appl. Phys. Lett. **126**, 044001 (2025); doi: 10.1063/5.0249115

Submitted: 15 November 2024 · Accepted: 12 January 2025 ·

Published Online: 27 January 2025



View Online



Export Citation



CrossMark

Liang Bin,¹ Dong-Xuan Zhang,² Lei Chen,¹ Yi-Hao Kang,² Zhi-Rong Zhong,^{1,a)} Qi-Ping Su,^{2,a)} and Chui-Ping Yang^{2,a)}

AFFILIATIONS

¹Department of Physics, Fuzhou University, Fuzhou 350002, China

²School of Physics, Hangzhou Normal University, Hangzhou 311121, China

^{a)}Authors to whom correspondence should be addressed: zhirz@fzu.edu.cn; sqp@hznu.edu.cn; and yangcp@hznu.edu.cn

ABSTRACT

The transfer of quantum entangled states is of fundamental interest in quantum physics and plays an important role in quantum information processing, quantum communication, and quantum technology. Here, we propose a scheme to transfer quantum entangled states of two photonic qubits by utilizing four microwave cavities coupled to a superconducting qutrit (a three-level quantum system). The photonic qubits are encoded using two orthogonal eigenstates of the photon-number parity operator with eigenvalues ± 1 , which allows for various encodings for the photonic qubits. The employment of four cavities at distinct frequencies effectively reduces the inter-cavity crosstalk. The utilization of only a single superconducting qutrit as the coupler significantly reduces the circuit resources. The entanglement transfer can be completed in just one step, making this scheme remarkably efficient. During the state transfer process, the third energy level of the coupler qutrit remains unoccupied, and thus decoherence from this level is diminished. Our numerical simulations demonstrate that within current circuit quantum electrodynamics technology, one can achieve high-fidelity transfer of the entangled states of two photonic qubits encoded via squeezed vacuum states and cat states. Our scheme possesses generality and can be applied to accomplish the same task in a variety of physical systems.

© 2025 Author(s). All article content, except where otherwise noted, is licensed under a Creative Commons Attribution (CC BY) license (<https://creativecommons.org/licenses/by/4.0/>). <https://doi.org/10.1063/5.0249115>

Circuit quantum electrodynamics (QED) is an advanced field that delves into the interplay between light and matter, leveraging the interaction between superconducting (SC) qubits and microwave cavities to explore the fundamental physical principles. Over the past decade, circuit QED has emerged as one of the promising platforms for quantum computation and quantum information processing (QIP).^{1–13} SC qubits have experienced significant advancements in recent years, as evidenced by remarkable improvements in their coherence time^{14–18} and the flexibility of their energy-level rapid tuning.^{19–21} These advancements have made SC qubits as key elements in building quantum computers based on circuit QED. Over the last decades, a number of theoretical proposals have been put forward for transferring quantum states among SC qubits based on circuit QED.^{1,22–26} Experiments have not only demonstrated the successful transfer of quantum coherent states between two SC qubits via a microwave cavity²⁷ but also have achieved the transfer of quantum states in SC

qubits chain.²⁸ Moreover, they have successfully implemented the quantum entanglement swapping in a SC circuit.²⁹

Recently, the application of photonic qubits has attracted widespread attention within the fields of quantum computing and communication. Experimental realization of a microwave cavity with a high-quality factor has been achieved. Specifically, a one-dimensional microwave cavity achieves a quality factor of approximately $Q \sim 10^6$,^{30–35} whereas the quality factor of a three-dimensional microwave cavity is about $Q \sim 3.5 \times 10^7$.^{36–38} The lifetime of photons in microwave cavities is comparable to that of SC qubits.³⁹ Therefore, high-quality-factor microwave cavities or resonators serve as an integral component in QIP and play dual roles as an efficient quantum channel for information transfer^{1–3,40} and as a robust quantum memory.^{39,41}

Photonic qubits, in contrast to SC qubits, are characterized by a more expansive Hilbert space, allowing for a variety of encoding

methods. The expanded Hilbert space of photonic qubits significantly augments their ability to represent a broader array of computational basis states and enhances their storage capacity for quantum information. Different encodings offer distinct advantages, each optimized for various applications within the field of QIP. Photonic qubits can be encoded in a variety of ways, including being encoded by a single-photon state, a vacuum state, a coherent state, or a cat state. The photonic qubits encoded by single-photon and vacuum states are easy to operate;⁴² they exhibit robustness against single-photon loss with encoding via coherent states,⁴³ and can be used for quantum error correction through encoding based on cat states.⁴⁴

Numerous methods have been proposed to implement single-qubit,^{45–50} two-qubit,^{51–55} and even multi-qubit gates with photonic qubits.^{56–66} Moreover, various methods have been proposed for the preparation of different types of entangled states using photonic qubits.^{67–84} Additionally, significant progress has been made in transferring entangled states between matter qubits and photonic coherent-state qubits,⁸⁵ and between photonic discrete-variable qubits and photonic continuous-variable qubits.⁸⁶ In experiments, successful simulations of coherent transfer of single photons have been achieved.⁸⁷

The transfer of quantum entangled states is of fundamental interest in quantum physics and plays an important role in quantum information processing, quantum communication, and quantum technology. Previous studies^{85,86} have employed coherent states, vacuum states, and single-photon states for encoding photonic qubits in the entanglement transfer. Quantum communications and QIP can benefit from the different encodings of photonic qubits in the entanglement transfer. The photonic qubits considered in this paper, which are encoded via two arbitrary orthogonal eigenstates $|\varphi_e\rangle$ and $|\varphi_o\rangle$ of the photon-number parity operator $\hat{\pi} = e^{i\pi\hat{a}^\dagger\hat{a}}$ can offer a remarkably rich array of encodings, including both discrete-variable encoding and continuous-variable encoding. Here, \hat{a}^\dagger (\hat{a}) is the photon-creation (annihilation) operator.

With the above-mentioned encoding, we propose a one-step approach for transferring quantum entangled states of two photonic qubits from two microwave cavities to the other two microwave cavities, i.e.,

$$(a|\varphi_e\rangle_1|\varphi_e\rangle_2 + b|\varphi_o\rangle_1|\varphi_o\rangle_2)|0\rangle_3|0\rangle_4 \rightarrow |0\rangle_1|0\rangle_2(a|\varphi_e\rangle_3|\varphi_e\rangle_4 + b|\varphi_o\rangle_3|\varphi_o\rangle_4), \quad (1)$$

where $|0\rangle$ is the vacuum state, the subscripts 1 and 2 represent two microwave cavities, while the subscripts 3 and 4 represent the other two microwave cavities. Here, a and b are normalized complex numbers with $|a|^2 + |b|^2 = 1$, and the transferred state is a maximally entangled state for $a = b = \frac{1}{\sqrt{2}}$. The state transfer is achieved by four microwave cavities coupled to a SC qutrit. This proposal has several advantages: (i) Since the photonic qubits are encoded via two arbitrary orthogonal eigenstates of the photon-number parity operator, this proposal allows for various encodings for the photonic qubits. (ii) The employment of four cavities with different frequencies effectively reduces the inter-cavity crosstalk. (iii) The utilization of only a single SC qutrit as the coupler significantly reduces the circuit resources. (iv) The entanglement transfer can be completed in just one step, making this scheme remarkably efficient. (v) During the state transfer process, the third energy level of the coupler qutrit remains unoccupied and thus decoherence from this level is diminished.

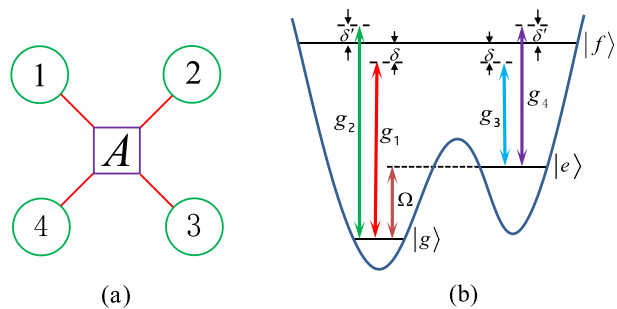


FIG. 1. (a) Schematic diagram of four microwave cavities and a SC qutrit. Each circle represents a microwave cavity, while the square A in the middle represents the SC qutrit. (b) Cavity 1 (2) is dispersively coupled to the $|g\rangle \leftrightarrow |f\rangle$ transition of the qutrit with coupling constant g_1 (g_2) and detuning δ (δ'), while cavity 3 (4) is dispersively coupled to the $|e\rangle \leftrightarrow |f\rangle$ transition of the qutrit with coupling constant g_3 (g_4) and detuning δ (δ'). Meanwhile, a microwave pulse with Rabi frequency Ω is applied to the qutrit, resonant with the transition between the two levels $|g\rangle$ and $|e\rangle$ [Fig. 1(b)].

Consider a system consisting of four cavities coupled to a common SC qutrit [Fig. 1(a)]. The three levels of the qutrit are labeled as $|g\rangle$, $|e\rangle$, and $|f\rangle$. Assume that cavity 1 (2) is dispersively coupled to the $|g\rangle \leftrightarrow |f\rangle$ transition of the qutrit with coupling constant g_1 (g_2) and detuning δ (δ'), while cavity 3 (4) is dispersively coupled to the $|e\rangle \leftrightarrow |f\rangle$ transition of the qutrit with coupling constant g_3 (g_4) and detuning δ (δ'). Meanwhile, a microwave pulse with Rabi frequency Ω is applied to the qutrit, resonant with the transition between the two levels $|g\rangle$ and $|e\rangle$ [Fig. 1(b)].

The Hamiltonian, in the interaction picture and after applying the rotating-wave approximation, is described by (assuming $\hbar = 1$)

$$H_I = g_1 e^{i\delta t} \hat{a}_1 |f\rangle \langle g| + g_2 e^{i\delta' t} \hat{a}_2 |f\rangle \langle g| + g_3 e^{i\delta t} \hat{a}_3 |f\rangle \langle e| + g_4 e^{i\delta' t} \hat{a}_4 |f\rangle \langle e| + \Omega |e\rangle \langle g| + \text{H.c.}, \quad (2)$$

where \hat{a}_1 , \hat{a}_2 , \hat{a}_3 , and \hat{a}_4 represent the photon annihilation operators of cavities 1, 2, 3, and 4, respectively; $\delta = \omega_{fg} - \omega_1 = \omega_{fe} - \omega_3 > 0$ and $\delta' = \omega_{fg} - \omega_2 = \omega_{fe} - \omega_4 < 0$. Here, ω_{fg} , ω_{fe} , and ω_{eg} are, respectively, the $|g\rangle \leftrightarrow |f\rangle$ transition frequency, the $|e\rangle \leftrightarrow |f\rangle$ transition frequency, and the $|g\rangle \leftrightarrow |e\rangle$ transition frequency of the qutrit; while ω_1 , ω_2 , ω_3 , and ω_4 are, respectively, the frequencies of cavities 1, 2, 3, and 4.

Under the large detuning conditions $\delta \gg g_1, g_3$ and $\delta' \gg g_2, g_4$, the Raman coupling between the qutrit's energy levels $|g\rangle$ and $|e\rangle$ can be induced by the cavity pairs (1, 3) and (2, 4) due to the adiabatic elimination of the intermediate energy level $|f\rangle$. When $\frac{|\delta - \delta'|}{|\delta^{-1} + \delta'^{-1}|} \gg (g_1 g_2, g_1 g_4, g_2 g_3, g_3 g_4)$, there is no interaction between the cavity pairs (1, 2), (1, 4), (2, 3), and (3, 4) induced by the qutrit. Additionally, assume that the detunings δ and δ' significantly exceed the Rabi frequency Ω , such that the influence of the pulse on the Raman transition is negligible. Thus, the Hamiltonian (2) will be⁸⁸

$$H = -2G_1 \hat{a}_1^\dagger \hat{a}_1 |g\rangle \langle g| - 2G_2 \hat{a}_2^\dagger \hat{a}_2 |g\rangle \langle g| - 2G_3 \hat{a}_3^\dagger \hat{a}_3 |e\rangle \langle e| - 2G_4 \hat{a}_4^\dagger \hat{a}_4 |e\rangle \langle e| - 2G_{13} (\hat{a}_1 \hat{a}_3^\dagger |e\rangle \langle g| + \hat{a}_1^\dagger \hat{a}_3 |g\rangle \langle e|) - 2G_{24} (\hat{a}_2 \hat{a}_4^\dagger |e\rangle \langle g| + \hat{a}_2^\dagger \hat{a}_4 |g\rangle \langle e|) + \Omega \sigma_x, \quad (3)$$

where $\sigma_x = |e\rangle\langle g| + |g\rangle\langle e|$, $G_1 = g_1^2/(2\delta)$, $G_2 = g_2^2/(2\delta')$, $G_3 = g_3^2/(2\delta)$, $G_4 = g_4^2/(2\delta')$, $G_{13} = g_1g_3/(2\delta)$, and $G_{24} = g_2g_4/(2\delta')$. In Eq. (3), the first (second) line describes the Stark shifts of the energy level $|g\rangle$ ($|e\rangle$), which are dependent on the photon number. Meanwhile, the third line and the fourth line describe the coherent coupling between $|g\rangle$ and $|e\rangle$, caused by the cavity pair (1, 3) and the cavity pair (2, 4), respectively.

The operators corresponding to the SC qutrit in Eq. (3) can be expressed as $|g\rangle\langle g| = (I + \tilde{\sigma}^\dagger + \tilde{\sigma}^-)/2$, $|e\rangle\langle e| = (I - \tilde{\sigma}^\dagger - \tilde{\sigma}^-)/2$, $|e\rangle\langle g| = (\tilde{\sigma}_z + \tilde{\sigma}^\dagger - \tilde{\sigma}^-)/2$, $|g\rangle\langle e| = (\tilde{\sigma}_z - \tilde{\sigma}^\dagger + \tilde{\sigma}^-)/2$, and $\sigma_x = \tilde{\sigma}_z$, where $\tilde{\sigma}_z = |+\rangle\langle +| - |-\rangle\langle -|$, $\tilde{\sigma}^\dagger = |+\rangle\langle -|$, and $\tilde{\sigma}^- = |-\rangle\langle +|$. Here, $|+\rangle = (|g\rangle + |e\rangle)/\sqrt{2}$ and $|-\rangle = (|g\rangle - |e\rangle)/\sqrt{2}$. Using the above-mentioned expressions, Eq. (3) can be rewritten as

$$\begin{aligned} H = & -G_1\hat{a}_1^\dagger\hat{a}_1(I + \tilde{\sigma}^\dagger + \tilde{\sigma}^-) - G_2\hat{a}_2^\dagger\hat{a}_2(I + \tilde{\sigma}^\dagger + \tilde{\sigma}^-) \\ & - G_3\hat{a}_3^\dagger\hat{a}_3(I - \tilde{\sigma}^\dagger - \tilde{\sigma}^-) - G_4\hat{a}_4^\dagger\hat{a}_4(I - \tilde{\sigma}^\dagger - \tilde{\sigma}^-) \\ & - G_{13}\hat{a}_1^\dagger\hat{a}_3^\dagger(\tilde{\sigma}_z + \tilde{\sigma}^\dagger - \tilde{\sigma}^-) - G_{13}\hat{a}_1^\dagger\hat{a}_3(\tilde{\sigma}_z - \tilde{\sigma}^\dagger + \tilde{\sigma}^-) \\ & - G_{24}\hat{a}_2^\dagger\hat{a}_4^\dagger(\tilde{\sigma}_z + \tilde{\sigma}^\dagger - \tilde{\sigma}^-) - G_{24}\hat{a}_2^\dagger\hat{a}_4(\tilde{\sigma}_z - \tilde{\sigma}^\dagger + \tilde{\sigma}^-) + \Omega\tilde{\sigma}_z. \end{aligned} \quad (4)$$

After applying the unitary transformation $U = e^{iH_0t}$ with $H_0 = \Omega\tilde{\sigma}_z$ and performing a unitary transformation e^{-iH_0t} to return to the original interaction picture, we obtain from Eq. (4) (see the [supplementary material](#))

$$\begin{aligned} \tilde{H} = & -(G_1\hat{a}_1^\dagger\hat{a}_1 + G_2\hat{a}_2^\dagger\hat{a}_2 + G_3\hat{a}_3^\dagger\hat{a}_3 + G_4\hat{a}_4^\dagger\hat{a}_4) + \Omega\tilde{\sigma}_z \\ & - G_{13}(\hat{a}_1^\dagger\hat{a}_3 + \hat{a}_3^\dagger\hat{a}_1)\tilde{\sigma}_z - G_{24}(\hat{a}_2^\dagger\hat{a}_4 + \hat{a}_4^\dagger\hat{a}_2)\tilde{\sigma}_z. \end{aligned} \quad (5)$$

After applying the additional unitary transformation $\tilde{U} = e^{i\tilde{H}_0t}$ with $\tilde{H}_0 = -(G_1\hat{a}_1^\dagger\hat{a}_1 + G_2\hat{a}_2^\dagger\hat{a}_2 + G_3\hat{a}_3^\dagger\hat{a}_3 + G_4\hat{a}_4^\dagger\hat{a}_4) + \Omega\tilde{\sigma}_z$, the Hamiltonian in the second new interaction picture will be (see the [supplementary material](#))

$$H_e = -G(\hat{a}_1^\dagger\hat{a}_3 + \hat{a}_3^\dagger\hat{a}_1)\tilde{\sigma}_z + G(\hat{a}_2^\dagger\hat{a}_4 + \hat{a}_4^\dagger\hat{a}_2)\tilde{\sigma}_z, \quad (6)$$

where we have assumed

$$G_1 = G_3, \quad G_2 = G_4, \quad G = G_{13} = -G_{24}. \quad (7)$$

In this work, the two logic states $|0\rangle$ and $|1\rangle$ of a photonic qubit are encoded by two arbitrary orthogonal eigenstates of the photon-number parity operator $\hat{\pi} = e^{i\pi\hat{a}^\dagger\hat{a}}$, denoted as $|\varphi_e\rangle$ with the eigenvalue of 1 and $|\varphi_o\rangle$ with the eigenvalue of -1, i.e.,

$$\begin{aligned} |0\rangle &= |\varphi_e\rangle = \sum_p d_p |p\rangle, \\ |1\rangle &= |\varphi_o\rangle = \sum_q d_q |q\rangle, \end{aligned} \quad (8)$$

where the coefficients d_p and d_q satisfy the normalization conditions $\sum_p |d_p|^2 = \sum_q |d_q|^2 = 1$. The state $|p\rangle$ corresponds to a Fock state within a cavity, representing an arbitrary even count p of photons; while the state $|q\rangle$ represents a Fock state within the cavity, containing an arbitrary odd count q of photons. It is easy to see that the states $|\varphi_e\rangle$ and $|\varphi_o\rangle$ are mutually orthogonal. By applying the operator $\hat{\pi}$ to the states $|\varphi_e\rangle$ and $|\varphi_o\rangle$, one has $\hat{\pi}|\varphi_e\rangle = |\varphi_e\rangle$ and $\hat{\pi}|\varphi_o\rangle = -|\varphi_o\rangle$. This confirms that the states $|\varphi_e\rangle$ and $|\varphi_o\rangle$ are eigenstates of the photon-number parity operator $\hat{\pi} = e^{i\pi\hat{a}^\dagger\hat{a}}$, with corresponding eigenvalues +1 and -1, respectively.

As shown in the physical setup depicted in [Fig. 1\(a\)](#), consider a SC qutrit initially in the state $|+\rangle$, which is prepared by applying a microwave pulse resonant with the $|g\rangle \rightarrow |e\rangle$ transition of the qutrit in the state $|g\rangle$. The pulse duration is $\frac{\pi}{4\Omega}$, and the initial phase of the pulse is $-\frac{\pi}{2}$. It is noted that the initial state $|+\rangle$ of the SC qutrit remains unaffected by the Hamiltonian (6). Thus, the part of the Hamiltonian (6) related to the SC qutrit can be disregarded. Hence, from Eq. (6), we obtain

$$H_e = -G(\hat{a}_1^\dagger\hat{a}_3 + \hat{a}_3^\dagger\hat{a}_1) + G(\hat{a}_2^\dagger\hat{a}_4 + \hat{a}_4^\dagger\hat{a}_2). \quad (9)$$

Cavities 1 and 2 are initially in the entangled state $a|\varphi_e\rangle_1|\varphi_e\rangle_2 + b|\varphi_o\rangle_1|\varphi_o\rangle_2$, whereas cavities 3 and 4 are initially in the vacuum state $|0\rangle_3|0\rangle_4$. Here, the subscripts 1, 2, 3, and 4 represent cavities 1, 2, 3, and 4, respectively. The initial state of the cavity system is thus given by

$$|\psi(0)\rangle = (a|\varphi_e\rangle_1|\varphi_e\rangle_2 + b|\varphi_o\rangle_1|\varphi_o\rangle_2)|0\rangle_3|0\rangle_4. \quad (10)$$

Under the Hamiltonian H_e of Eq. (9), the state of the cavity system will evolve to the following state (see the [supplementary material](#)):

$$\begin{aligned} |\psi\rangle = & a|0\rangle_1|0\rangle_2 \sum_p d_p e^{i\frac{p}{2}\pi} |p\rangle_3 \sum_p d_p e^{-i\frac{p}{2}\pi} |p\rangle_4 \\ & + b|0\rangle_1|0\rangle_2 \sum_q d_q e^{i\frac{q}{2}\pi} |q\rangle_3 \sum_q d_q e^{-i\frac{q}{2}\pi} |q\rangle_4. \end{aligned} \quad (11)$$

Note that the Hamiltonian (6) and (9) are expressed in the second new interaction picture. Thus, in order to complete the entangled states transfer in the original interaction picture, one needs to apply a unitary transformation $e^{-i\tilde{H}_0t}$ to return to the original interaction picture, the state (11) becomes (see the [supplementary material](#))

$$|\psi\rangle_f = e^{-i\phi_0}|0\rangle_1|0\rangle_2(a|\varphi_e\rangle_3|\varphi_e\rangle_4 + b|\varphi_o\rangle_3|\varphi_o\rangle_4), \quad (12)$$

where $\phi_0 = \Omega\pi/(2G)$ is a global phase that can be ignored.

Based on the above-mentioned description, the following can be seen:

- Each photonic qubit is encoded by two arbitrary orthogonal eigenstates $|\varphi_e\rangle$ (with eigenvalue 1) and $|\varphi_o\rangle$ (with eigenvalue -1) of the photon-number parity operator $\hat{\pi} = e^{i\pi\hat{a}^\dagger\hat{a}}$ of a cavity, which allows for various encodings of the photonic qubits. For instance, they can have the following encodings: (i) $|\varphi_e\rangle$ is the vacuum state $|0\rangle$ and $|\varphi_o\rangle$ is the single-photon state $|1\rangle$; (ii) $|\varphi_e\rangle$ is an even cat state $|cat\rangle$ with $|cat\rangle = \mathcal{N}_+ (|\alpha\rangle + |-\alpha\rangle)$, and $|\varphi_o\rangle$ is an odd cat state $|\overline{cat}\rangle$ with $|\overline{cat}\rangle = \mathcal{N}_- (|\alpha\rangle - |-\alpha\rangle)$, where \mathcal{N}_+ (\mathcal{N}_-) is a normalization factor; (iii) $|\varphi_e\rangle$ is an even Fock state $|2m\rangle$, and $|\varphi_o\rangle$ is an odd Fock state $|2n+1\rangle$; and (iv) $|\varphi_e\rangle$ is a squeezed vacuum state $|\xi\rangle$ with $|\xi\rangle$ being a superposition state of Fock states with even-number photons, and $|\varphi_o\rangle$ is an odd cat state $|\overline{cat}\rangle$, and so on.
- The entanglement transfer is completed in just one step.
- During the state transfer process, the third energy level $|f\rangle$ of the coupler qutrit is not occupied, and thus decoherence from this level is diminished.
- The utilization of only a single SC qutrit as the coupler significantly reduces the circuit resources.
- The operation time is (see the [supplementary material](#))

$$t = \pi/(2G), \quad (13)$$

which should be much shorter than both the decoherence time of the qutrit and the cavity decay time, ensuring that the system dissipation is negligibly small during the state transfer.

(vi) The above-mentioned condition (7) turns out into

$$g_1 = g_3, \quad g_2 = g_4, \quad g_1 g_3 / \delta = -g_2 g_4 / \delta', \quad (14)$$

which can be satisfied by adjusting the cavity frequency, the qutrit's energy-level spacings, and the coupling strengths (e.g., through varying the capacitance between the SC qutrit and the cavities).

In the following, we present a discussion on the experimental feasibility of transferring quantum entangled states of two photonic qubits from two cavities to the other two cavities by employing four 3D microwave cavities coupled to a SC flux qutrit (Fig. 2).^{15,89,90} Here, each photonic qubit is encoded via a squeezed vacuum state $|\xi\rangle$ and a cat state $|\text{cat}\rangle$. As mentioned previously, the encoding with a squeezed vacuum state $|\xi\rangle$ and a cat state $|\text{cat}\rangle$ is an example for the encoding states $|\varphi_e\rangle$ and $|\varphi_o\rangle$.

When considering the unwanted cavities-qutrit interactions, the unwanted pulse-induced interactions, and the inter-cavity crosstalk, the Hamiltonian (2) is modified as $H' = H_1 + \delta H + \epsilon_1 + \epsilon_2$. Here, δH represents the unwanted inter-cavity crosstalk, which can be expressed as

$$\begin{aligned} \delta H = & g_{12} e^{-i\delta_{12}t} \hat{a}_1 \hat{a}_2^\dagger + g_{13} e^{-i\delta_{13}t} \hat{a}_1 \hat{a}_3^\dagger \\ & + g_{14} e^{-i\delta_{14}t} \hat{a}_1 \hat{a}_4^\dagger + g_{23} e^{-i\delta_{23}t} \hat{a}_2 \hat{a}_3^\dagger \\ & + g_{24} e^{-i\delta_{24}t} \hat{a}_2 \hat{a}_4^\dagger + g_{34} e^{-i\delta_{34}t} \hat{a}_3 \hat{a}_4^\dagger + \text{H.c.} \end{aligned} \quad (15)$$

Here, g_{kl} and $\delta_{kl} = \omega_k - \omega_l$ represent the coupling strength and frequency detuning between cavities k and l , respectively, ($kl = 12, 13, 14, 23, 24, 34$); and ϵ_1 represents the unwanted pulse-induced $|e\rangle \leftrightarrow |f\rangle$ transition of the SC qutrit, which can be expressed as

$$\epsilon_1 = \Omega_{fe} e^{i\delta_p t} |f\rangle \langle e| + \text{H.c.}, \quad (16)$$

where $\delta_p = \omega_{fe} - \omega_{eg}$, and Ω_{fe} represents the Rabi frequency of the pulse (Fig. 3). In addition, ϵ_2 represents the unwanted cavity-induced $|g\rangle \leftrightarrow |e\rangle$ transition of the SC qutrit, which can be expressed as

$$\epsilon_2 = \tilde{g}_3 e^{i\tilde{\delta}t} \hat{a}_3 |e\rangle \langle g| + \tilde{g}_4 e^{i\tilde{\delta}'t} \hat{a}_4 |e\rangle \langle g| + \text{H.c.}, \quad (17)$$

where the first term (the second term) describes the unwanted coupling between cavity 3 (cavity 4) and the $|g\rangle \leftrightarrow |e\rangle$ transition of the qutrit with coupling constant \tilde{g}_3 (\tilde{g}_4) and detuning $\tilde{\delta} = \omega_{eg} - \omega_3$

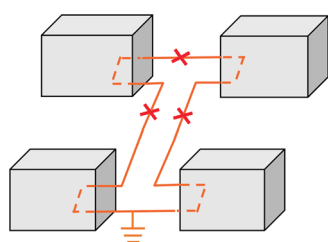


FIG. 2. Schematic circuit of four 3D microwave cavities coupled to a SC flux qutrit. Each box represents a 3D microwave cavity, and the loop with three Josephson junctions represents a SC flux qutrit.

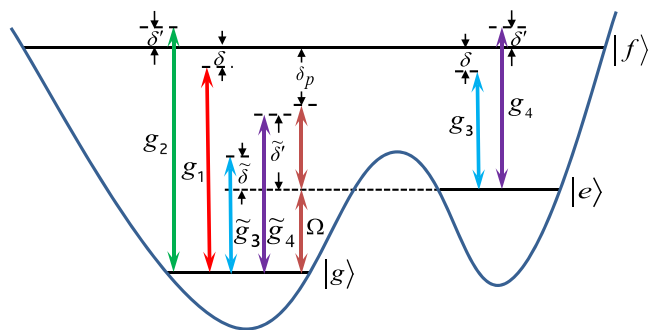


FIG. 3. Illustration of the unwanted coupling between cavity 3 (cavity 4) and the $|g\rangle \leftrightarrow |e\rangle$ transition of the qutrit with coupling constant \tilde{g}_3 (\tilde{g}_4) and detuning $\tilde{\delta} = \omega_{eg} - \omega_3$ ($\tilde{\delta}' = \omega_{eg} - \omega_4$) as well as the unwanted pulse-induced $|e\rangle \leftrightarrow |f\rangle$ transition of the SC qutrit with the Rabi frequency Ω_{fe} and detuning $\delta_p = \omega_{fe} - \omega_{eg}$.

($\tilde{\delta}' = \omega_{eg} - \omega_4$) (Fig. 3). Due to $\omega_{fg} \gg \omega_{eg}$, ω_{eg} , the $|g\rangle \leftrightarrow |f\rangle$ transition induced by the cavities 3 and 4 or the pulse can be neglected, and thus is not considered in our numerical simulations.

When considering the dissipation of the cavities and the decoherence of the SC qutrit, the master equation for the dissipative system is determined by

$$\begin{aligned} \frac{d\rho}{dt} = & -i[H', \rho] + \sum_{j=1}^4 \kappa_j \mathcal{L}[\hat{a}_j] + \gamma_{eg} \mathcal{L}[\sigma_{eg}^-] \\ & + \gamma_{fe} \mathcal{L}[\sigma_{fe}^-] + \gamma_{fg} \mathcal{L}[\sigma_{fg}^-] \\ & + \gamma_{\varphi,e} (\sigma_{ee} \rho_{ee} - \sigma_{ee} \rho / 2 - \rho \sigma_{ee} / 2) \\ & + \gamma_{\varphi,f} (\sigma_{ff} \rho_{ff} - \sigma_{ff} \rho / 2 - \rho \sigma_{ff} / 2), \end{aligned} \quad (18)$$

where H' is the modified Hamiltonian given earlier, $\sigma_{eg}^- = |g\rangle \langle e|$, $\sigma_{fe}^- = |e\rangle \langle f|$, $\sigma_{fg}^- = |g\rangle \langle f|$, $\sigma_{ee}^- = |e\rangle \langle e|$, $\sigma_{ff}^- = |f\rangle \langle f|$, and $\mathcal{L}[\Lambda] = \Lambda \rho \Lambda^\dagger - \Lambda^\dagger \Lambda \rho / 2 - \rho \Lambda^\dagger \Lambda / 2$, with $(\Lambda = \hat{a}_1, \hat{a}_2, \hat{a}_3, \hat{a}_4, \sigma_{eg}^-, \sigma_{fe}^-, \sigma_{fg}^-)$. Additionally, κ_j is the decay rate of cavity j ($j = 1, 2, 3, 4$); γ_{eg} is the energy relaxation rate of the level $|e\rangle$ for the decay path $|e\rangle \rightarrow |g\rangle$; γ_{fe} (γ_{fg}) is the energy relaxation rate of the level $|f\rangle$ for the decay path $|f\rangle \rightarrow |e\rangle$ ($|f\rangle \rightarrow |g\rangle$), and $\gamma_{\varphi,e}$ ($\gamma_{\varphi,f}$) is the dephasing rate of the level $|e\rangle$ ($|f\rangle$) of the qutrit.

The fidelity of the quantum entangled state transfer can be expressed as

$$F = \sqrt{\langle \psi_{\text{id}} | \rho | \psi_{\text{id}} \rangle}. \quad (19)$$

Here, $|\psi_{\text{id}}\rangle$ represents the ideal output state, which can be expressed as $|\psi_{\text{id}}\rangle = |0\rangle_1 |0\rangle_2 \frac{1}{\sqrt{2}} (|\xi\rangle_3 |\xi\rangle_4 + |\text{cat}\rangle_3 |\text{cat}\rangle_4) |+\rangle$ according to Eq. (12) with $a = b = \frac{1}{\sqrt{2}}$ and because the initial state $|+\rangle$ of the SC qutrit remains unchanged during the state transfer. Meanwhile, ρ is the density operator that is calculated by solving the master equation (18), which takes into account the system's dissipation, the unwanted interactions, and the inter-cavity crosstalk.

Additional parameters employed in our numerical simulations are as follows: (i) $\gamma_{eg}^{-1} = T \text{ } \mu\text{s}$, $\gamma_{fg}^{-1} = T \text{ } \mu\text{s}$, $\gamma_{fe}^{-1} = T \text{ } \mu\text{s}$, $\gamma_{\varphi,e}^{-1} = \gamma_{\varphi,f}^{-1} = T/2 \text{ } \mu\text{s}$; (ii) $\kappa_1 = \kappa_2 = \kappa_3 = \kappa_4 = \kappa$; (iii) $g_{12} = g_{13} = g_{14} = g_{23} = g_{24} = g_{34} = g_c$; (iv) $\alpha = 0.5$; (v) $\tilde{g}_3 = g_3$, $\tilde{g}_4 = g_4$; (vi) $\Omega/2\pi = \Omega_{fe}/2\pi = 50 \text{ MHz}$; and (vii) $\xi = 0.5$. Note that the coupling

TABLE I. Parameters used in the numerical simulation.

$\omega_{eg}/(2\pi) = 5.5$ GHz	$\omega_{fe}/(2\pi) = 10.5$ GHz	$\omega_{fg}/(2\pi) = 16$ GHz
$g_1/(2\pi) = 55$ MHz	$g_2/(2\pi) = 70$ MHz	$g_3/(2\pi) = 55$ MHz
$g_4/(2\pi) = 70$ MHz	$\delta/2\pi = 0.8$ GHz	$\delta'/2\pi = -1.3$ GHz
$\omega_1/2\pi = 15.2$ GHz	$\omega_2/2\pi = 17.3$ GHz	$\omega_3/2\pi = 9.7$ GHz
$\omega_4/2\pi = 11.8$ GHz	$\delta_{12}/2\pi = -2.1$ GHz	$\delta_{13}/2\pi = 5.5$ GHz
$\delta_{14}/2\pi = 3.4$ GHz	$\delta_{23}/2\pi = -7.6$ GHz	$\delta_{24}/2\pi = 5.5$ GHz
$\delta_{34}/2\pi = -2.1$ GHz	$\delta_p/2\pi = 5$ GHz	$\tilde{\delta}/2\pi = -4.2$ GHz
$\tilde{\delta}/2\pi = -6.3$ GHz		

strength between a SC flux qubit and a microwave cavity can reach $2\pi \times 636$ MHz.^{91,92}

By solving the master equation (18), we calculate the fidelity of entangled state transfer with the parameters chosen above and in Table I. By setting $T = 40$ μ s in numerical simulations, we plot Fig. 4, which shows how fidelity varies with κ^{-1} for $g_c = 0, 0.01g_{\max}$, and $0.1g_{\max}$, where $g_{\max} = \max\{g_1, g_2, g_3, g_4, \tilde{g}_3, \tilde{g}_4\}$. According to Fig. 4, we can observe that the fidelity exceeds 99.01% for $\kappa^{-1} \geq 40$ μ s and $g_c = 0.01g_{\max}$. It is worth noting that the inter-cavity crosstalk strength can be made $0.01g_{\max}$ by a prior design of the sample in experiments.⁶⁹ It is worth noting that the inter-cavity crosstalk strength can be made $0.01g_{\max}$ by a prior design of the sample in experiments,⁶⁹ and the decoherence times of the flux qutrit are achievable due to experimental reports showing decoherence times ranging from 70 μ s to 1 ms.^{15,91,93}

Based on the parameters in Table I, the operational time is estimated as 0.14 μ s, which is much shorter than both the decoherence time (20 – 40 μ s) of the qutrit and the dissipation time of the cavity (10 – 150 μ s) used in numerical simulations. For the cavity dissipation time $\kappa^{-1} = 40$ μ s, the quality factors of the four cavities are $Q_1 \sim 3.84 \times 10^6$, $Q_2 \sim 4.32 \times 10^6$, $Q_3 \sim 2.44 \times 10^6$, and $Q_4 \sim 2.96 \times 10^6$, which are achievable as a high $Q \sim 3.5 \times 10^7$ for a 3D microwave cavity has been demonstrated in experiments.^{36–38}

The above-mentioned analysis implies that high-fidelity transfer of quantum entangled states of two photonic qubits encoded by a

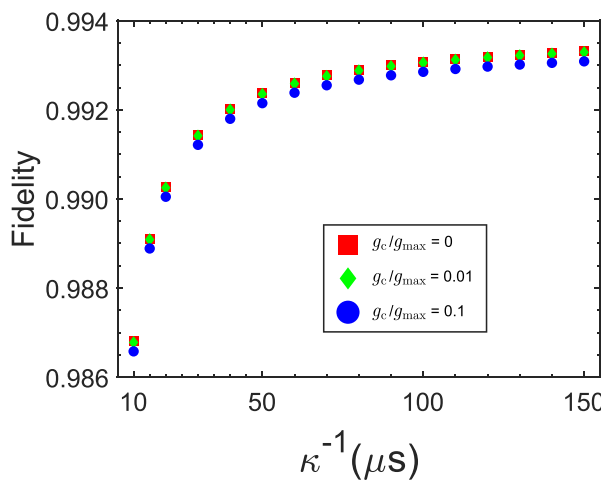


FIG. 4. Fidelity vs κ^{-1} for $g_c = 0, 0.01g_{\max}, 0.1g_{\max}$, and $T = 40$ μ s.

squeezed vacuum state $|\xi\rangle$ and a cat state $|\overline{cat}\rangle$ from two microwave cavities to the other two microwave cavities can be achieved within current circuit QED techniques. Our proposal is universal and can be applied to accomplish the same task in a variety of physical systems, which consists of a three-level artificial atom (e.g., a quantum dot, a NV center, a magnon, a superconducting qutrit with different types) coupled to four microwave or optical cavities.

See the of [supplementary material](#), subsection I, for the derivation of Eqs. (5) and (6); subsection II for the derivation of Eqs. (11)–(13); and subsection III for the analysis of fidelity under various experimental imperfections.

This work was partly supported by the National Natural Science Foundation of China (NSFC) (Grant Nos. 12074070, 11074062, 11374083, 11774076, and U21A20436), the National Key Research and Development Program of China (Grant No. 2024YFA1408900), the Natural Science Foundation of Fujian Province (Grant No. 2020J01471), and the Innovation Program for Quantum Science and Technology (Grant No. 2021ZD0301705).

AUTHOR DECLARATIONS

Conflict of Interest

The authors have no conflicts to disclose.

Author Contributions

Liang Bin: Conceptualization (lead); Writing – original draft (lead). **Dong-Xuan Zhang:** Software (equal); Writing – review & editing (equal). **Lei Chen:** Formal analysis (equal); Writing – review & editing (equal). **Yi-Hao Kang:** Software (equal); Writing – review & editing (equal). **Zhi-Rong Zhong:** Supervision (lead); Writing – review & editing (equal). **Qi-Ping Su:** Software (equal); Writing – review & editing (equal). **Chui-Ping Yang:** Project administration (lead); Supervision (lead); Writing – review & editing (equal).

DATA AVAILABILITY

The data that support the findings of this study are available from the corresponding authors upon reasonable request.

REFERENCES

- 1C. P. Yang, S. I. Chu, and S. Y. Han, “Possible realization of entanglement, logical gates, and quantum information transfer with superconducting-quantum-interference-device qubits in cavity QED,” *Phys. Rev. A* **67**(4), 042311 (2003).
- 2J. Q. You and F. Nori, “Quantum information processing with superconducting qubits in a microwave field,” *Phys. Rev. B* **68**(6), 064509 (2003).
- 3A. Blais, R. S. Huang, A. Wallraff, S. M. Girvin, and R. J. Schoelkopf, “Cavity quantum electrodynamics for superconducting electrical circuits: An architecture for quantum computation,” *Phys. Rev. A* **69**(6), 062320 (2004).
- 4J. Q. You and F. Nori, “Superconducting circuits and quantum information,” *Phys. Today* **58**(11), 42 (2005).
- 5J. Clarke and F. K. Wilhelm, “Superconducting quantum bits,” *Nature* **453**(7198), 1031 (2008).
- 6J. Q. You and F. Nori, “Atomic physics and quantum optics using superconducting circuits,” *Nature* **474**(7353), 589 (2011).
- 7Z. L. Xiang, S. Ashhab, J. Q. You, and F. Nori, “Hybrid quantum circuits: Superconducting circuits interacting with other quantum systems,” *Rev. Mod. Phys.* **85**(2), 623 (2013).

⁸X. Gu, A. F. Kockum, A. Miranowicz, Y. X. Liu, and F. Nori, "Microwave photonics with superconducting quantum circuits," *Phys. Rep.* **718-719**, 1 (2017).

⁹P. B. Li, Y. C. Liu, S. Y. Gao, Z. L. Xiang, P. Rabl, Y. F. Xiao, and F. L. Li, "Hybrid quantum device based on NV centers in diamond nanomechanical resonators plus superconducting waveguide cavities," *Phys. Rev. Appl.* **4**(4), 044003 (2015).

¹⁰Z. Y. Xue and Y. Hu, "Topological photonics on superconducting quantum circuits with parametric couplings," *Adv. Quantum Technol.* **4**, 2100017 (2021).

¹¹M. Cattaneo and G. S. Paraoanu, "Engineering dissipation with resistive elements in circuit quantum electrodynamics," *Adv. Quantum Technol.* **4**, 2100054 (2021).

¹²S. Shahmir, M. A. Khan, T. Abbas, S. H. Alvi, and R. Islam, "Multi-party entanglement generation through superconducting circuits," *Int. J. Theor. Phys.* **62**, 102 (2023).

¹³S. M. Arslan, S. Al-Kuwari, and T. Abbas, "Superdense coding using Bragg diffracted hyperentangled atoms," *IEEE J. Sel. Areas Commun.* **42**(7), 1950 (2024).

¹⁴R. Barends, J. Kelly, A. Megrant, D. Sank, E. Jeffrey, Y. Chen, Y. Yin, B. Chiaro, J. Mutus, C. Neill *et al.*, "Coherent Josephson qubit suitable for scalable quantum integrated circuits," *Phys. Rev. Lett.* **111**(8), 080502 (2013).

¹⁵F. Yan, S. Gustavsson, A. Kamal, J. Birenbaum, A. P. Sears, D. Hover, T. J. Gudmundsen, J. L. Yoder, T. P. Orlando, J. Clarke *et al.*, "The flux qubit revisited to enhance coherence and reproducibility," *Nat. Commun.* **7**(1), 12964 (2016).

¹⁶A. P. M. Place, L. V. H. Rodgers, P. Mundada, B. M. Smitham, M. Fitzpatrick, Z. Q. Leng, A. Premkumar, J. Bryon, A. Vrajitoarea, S. Sussman *et al.*, "New material platform for superconducting transmon qubits with coherence times exceeding 0.3 milliseconds," *Nat. Commun.* **12**(1), 1779 (2021).

¹⁷C. Wang, X. Li, H. Xu, Z. Li, J. Wang, Z. Yang, Z. Mi, X. Liang, T. Su, C. Yang *et al.*, "Towards practical quantum computers transmon qubit with a lifetime approaching 0.5 milliseconds," *npj Quantum Inf.* **8**(1), 3 (2022).

¹⁸A. Somoroff, Q. Ficheux, R. A. Mencia, H. N. Xiong, R. Kuzmin, and V. E. Manucharyan, "Millisecond coherence in a superconducting qubit," *Phys. Rev. Lett.* **130**(26), 267001 (2023).

¹⁹P. J. Leek, S. Filipp, P. Maurer, M. Baur, R. Bianchetti, J. M. Fink, M. Goppl, L. Steffen, and A. Wallraff, "Using sideband transitions for two-qubit operations in superconducting circuits," *Phys. Rev. B* **79**, 180511(R) (2009).

²⁰M. Neeley, M. Ansmann, R. C. Bialczak, M. Hofheinz, N. Katz, E. Lucero, A. O'Connell, H. Wang, A. N. Cleland, and J. M. Martinis, "Process tomography of quantum memory in a Josephson-phase qubit coupled to a two-level state," *Nat. Phys.* **4**(7), 523 (2008).

²¹G. Z. Sun, X. D. Wen, B. Mao, J. Chen, Y. Yu, P. H. Wu, and S. Y. Han, "Tunable quantum beam splitters for coherent manipulation of a solid-state tripartite qubit system," *Nat. Commun.* **1**(1), 51 (2010).

²²C. P. Yang, S. I. Chu, and S. Y. Han, "Quantum information transfer and entanglement with SQUID qubits in cavity QED: A dark-state scheme with tolerance for nonuniform device parameter," *Phys. Rev. Lett.* **92**(11), 117902 (2004).

²³Q. Q. Wu, J. Q. Liao, and L. M. Kuang, "Quantum state transfer between charge and flux qubits in circuit-QED," *Chin. Phys. Lett.* **25**(4), 1179 (2008).

²⁴Z. B. Feng, "Quantum state transfer between hybrid qubits in a circuit QED," *Phys. Rev. A* **85**(1), 014302 (2012).

²⁵C. P. Yang, Q. P. Su, and F. Nori, "Entanglement generation and quantum information transfer between spatially - separated qubits in different cavities," *New J. Phys.* **15**(11), 115003 (2013).

²⁶F. W. Strauch and C. J. Williams, "Theoretical analysis of perfect quantum state transfer with superconducting qubits," *Phys. Rev. B* **78**(9), 094516 (2008).

²⁷M. A. Sillanp, J. I. Park, and R. W. Simmonds, "Coherent quantum state storage and transfer between two phase qubits via a resonant cavity," *Nature* **449**(7161), 438 (2007).

²⁸X. Li, Y. Ma, J. Han, T. Chen, Y. Xu, W. Cai, H. Wang, Y. P. Song, Z. Y. Xue, Z. Q. Yin *et al.*, "Perfect quantum state transfer in a superconducting qubit chain with parametrically tunable couplings," *Phys. Rev. Appl.* **10**(5), 054009 (2018).

²⁹W. Ning, X. J. Huang, P. R. Han, H. Li, H. Deng, Z. B. Yang, Z. R. Zhong, Y. Xia, K. Xu, D. Zheng *et al.*, "Deterministic entanglement swapping in a superconducting circuit," *Phys. Rev. Lett.* **123**(6), 060502 (2019).

³⁰W. Chen, D. A. Bennett, V. Patel, and J. E. Lukens, "Substrate and process dependent losses in superconducting thin film resonators," *Supercond. Sci. Technol.* **21**(7), 075013 (2008).

³¹P. J. Leek, M. Baur, J. M. Fink, R. Bianchetti, L. Stefen, S. Filipp, and A. Wallraff, "Cavity quantum electrodynamics with separate photon storage and qubit read-out modes," *Phys. Rev. Lett.* **104**(10), 100504 (2010).

³²A. Megrant, C. Neill, R. Barends, B. Chiaro, Y. Chen, L. Feigl, J. Kelly, E. Lucero, M. Mariantoni, P. J. J. O'Malley *et al.*, "Planar superconducting resonators with internal quality factors above one million," *Appl. Phys. Lett.* **100**(11), 113510 (2012).

³³G. Calusine, A. Melville, W. Woods, R. Das, C. Stull, V. Bolkhovsky, D. Braje, D. Hover, D. K. Kim, X. Miloshi *et al.*, "Analysis and mitigation of interface losses in trenched superconducting coplanar waveguide resonators," *Appl. Phys. Lett.* **112**(6), 062601 (2018).

³⁴W. Woods, G. Calusine, A. Melville, A. Sevi, E. Golden, D. K. Kim, D. Rosenberg, J. L. Yoder, and W. D. Oliver, "Determining interface dielectric losses in superconducting coplanar waveguide resonators," *Phys. Rev. Appl.* **12**(1), 014012 (2019).

³⁵A. Melville, G. Calusine, W. Woods, K. Serniak, E. Golden, B. M. Niedzielski, D. K. Kim, A. Sevi, J. L. Yoder, E. A. Dauler *et al.*, "Comparison of dielectric loss in titanium nitride and aluminum superconducting resonators," *Appl. Phys. Lett.* **117**(12), 124004 (2020).

³⁶M. Reagor, W. Pfaff, C. Axline, R. W. Heeres, N. Ofek, K. Sliwa, E. Holland, C. Wang, J. Blumoff, K. Chou *et al.*, "A quantum memory with near - millisecond coherence in circuit QED," *Phys. Rev. B* **94**(1), 014506 (2016).

³⁷M. Kudra, J. Biznarova, A. Fadavi Roudsari, J. J. Burnett, D. Niepce, S. Gasparinetti, B. Wickman, and P. Delsing, "High quality three-dimensional aluminum microwave cavities," *Appl. Phys. Lett.* **117**(7), 070601 (2020).

³⁸A. Romanenko, R. Pilipenko, S. Zorzetti, D. Frolov, M. Awida, S. Belomestnykh, S. Posen, and A. Grassellino, "Three-dimensional superconducting resonators at $T < 20$ mK with photon lifetimes up to $\tau = 2$ s," *Phys. Rev. Appl.* **13**(3), 034032 (2020).

³⁹M. H. Devoret and R. J. Schoelkopf, "Superconducting circuits for quantum information: An outlook," *Science* **339**(6124), 1169 (2013).

⁴⁰F. Y. Zhang, Y. X. Zeng, Q. C. Wu, and C. P. Yang, "Cat-state encoding of a quantum information processor module with cavity-magnon system," *Appl. Phys. Lett.* **122**(8), 084001 (2023).

⁴¹M. Hofheinz, H. Wang, M. Ansmann, R. C. Bialczak, E. Lucero, M. Neeley, A. D. O'Connell, D. Sank, J. Wenner, J. M. Martinis, and A. N. Cleland, "Synthesizing arbitrary quantum states in a superconducting resonator," *Nature* **459**(7246), 546 (2009).

⁴²M. Hua, M. J. Tao, and F. G. Deng, "Universal quantum gates on microwave photons assisted by circuit quantum electrodynamics," *Phys. Rev. A* **90**(1), 012328 (2014).

⁴³M. O. Scully and W. E. Lamb, "Quantum theory of an optical maser. III. Theory of photoelectron counting statistics," *Phys. Rev.* **179**(2), 368 (1969).

⁴⁴N. Ofek, A. Petrenko, R. Heeres, P. Reinhold, Z. Leghtas, B. Vlastakis, Y. Liu, L. Frunzio, S. M. Girvin, L. Jiang *et al.*, "Extending the lifetime of a quantum bit with error correction in superconducting circuits," *Nature* **536**(7617), 441 (2016).

⁴⁵H. Jeong and M. S. Kim, "Efficient quantum computation using coherent states," *Phys. Rev. A* **65**(4), 042305 (2002).

⁴⁶T. C. Ralph, A. Gilchrist, and G. J. Milburn, "Quantum computation with optical coherent states," *Phys. Rev. A* **68**(4), 042319 (2003).

⁴⁷M. Mirrahimi, Z. Leghtas, V. V. Albert, S. Touzard, R. J. Schoelkopf, L. Jiang, and M. H. Devoret, "Dynamically protected cat-qubits: A new paradigm for universal quantum computation," *New J. Phys.* **16**(4), 045014 (2014).

⁴⁸S. E. Nigg, "Deterministic Hadamard gate for microwave cat-state qubits in circuit QED," *Phys. Rev. A* **89**(2), 022340 (2014).

⁴⁹R. W. Heeres, P. Reinhold, N. Ofek, L. Frunzio, L. Jiang, M. H. Devoret, and R. J. Schoelkopf, "Implementing a universal gate set on a logical qubit encoded in an oscillator," *Nat. Commun.* **8**(1), 94 (2017).

⁵⁰F. Morozko, A. Novitsky, A. Mikhalychev, and A. Karabchevsky, "On-chip polarization-encoded single-qubit gates with twisted waveguides," *Phys. Rev. Res.* **5**, 043155 (2023).

⁵¹J. Howard, A. Lidiak, C. Jameson, B. Basyildiz, K. Clark, T. Zhao, M. Bal, J. Long, D. P. Pappas, M. Singh, and Z. Gong, "Implementing two-qubit gates at the quantum speed limit," *Phys. Rev. Res.* **5**, 043194 (2023).

⁵²F. Riera-Sabat, P. Sekatski, and W. Dür, "Quantum computation with logical gates between hot systems," *Phys. Rev. Res.* **6**, 033101 (2024).

⁵³M. Chen, J. S. Tang, M. Cai, Y. Lu, F. Nori, and K. Xia, "High-dimensional two-photon quantum controlled phase-flip gate," *Phys. Rev. Res.* **6**, 033004 (2024).

⁵⁴C. P. Yang, Q. P. Su, S. B. Zheng, F. Nori, and S. Han, "Entangling two oscillators with arbitrary asymmetric initial states," *Phys. Rev. A* **95**(5), 052341 (2017).

⁵⁵Q. P. Su, Y. Zhang, L. Bin, and C. P. Yang, "Hybrid controlled-sum gate with one superconducting qutrit and one cat-state qutrit and application in hybrid entangled state preparation," *Phys. Rev. A* **105**, 042434 (2022).

⁵⁶P. M. Lu, J. Song, and Y. Xia, "Implementing a multi-qubit quantum phase gate encoded by photonic qubit," *Chin. Phys. Lett.* **27**(3), 030302 (2010).

⁵⁷M. Hua, M. J. Tao, and F. G. Deng, "Fast universal quantum gates on microwave photons with all-resonance operations in circuit QED," *Sci. Rep.* **5**(1), 9274 (2015).

⁵⁸J. X. Han, J. L. Wu, Y. Wang, Y. Y. Jiang, Y. Xian, and J. Song, "Multi-qubit phase gate on multiple resonators mediated by a superconducting bus," *Opt. Express* **28**(2), 1954 (2020).

⁵⁹Q. P. Su, Y. Zhang, L. Bin, and C. P. Yang, "Efficient scheme for realizing a multiplexed controlled phase gate with photonic qubits in circuit quantum electrodynamics," *Front. Phys.* **17**(5), 53505 (2022).

⁶⁰J. Fiurasek, "Linear-optics quantum Toffoli and Fredkin gates," *Phys. Rev. A* **73**(6), 062313 (2006).

⁶¹X. Zou, K. Li, and G. Guo, "Linear optical scheme for direct implementation of a nondestructive N-qubit controlled phase gate," *Phys. Rev. A* **74**(4), 044305 (2006).

⁶²T. C. Ralph, K. J. Resch, and A. Gilchrist, "Efficient Toffoli gates using qudits," *Phys. Rev. A* **75**(2), 022313 (2007).

⁶³H. R. Wei and G. L. Long, "Universal photonic quantum gates assisted by ancilla diamond nitrogen-vacancy centers coupled to resonators," *Phys. Rev. A* **91**(3), 032324 (2015).

⁶⁴H. L. Huang, W. S. Bao, T. Li, F. G. Li, X. Q. Fu, S. Zhang, H. L. Zhang, and X. Wang, "Deterministic linear optical quantum Toffoli gate," *Phys. Lett. A* **381**(33), 2673 (2017).

⁶⁵L. Dong, S. L. Wang, C. Cui, X. Geng, Q. Y. Li, H. K. Dong, X. M. Xiu, and Y. J. Gao, "Polarization Toffoli gate assisted by multiple degrees of freedom," *Opt. Lett.* **43**(19), 4635–4638 (2018).

⁶⁶B. Y. Xia, C. Cao, Y. H. Han, and R. Zhang, "Universal photonic three-qubit quantum gates with two degrees of freedom assisted by charged quantum dots inside single-sided optical microcavities," *Laser Phys.* **28**(9), 095201 (2018).

⁶⁷X. Y. Lu, G. L. Zhu, L. L. Zheng, and Y. Wu, "Entanglement and quantum superposition induced by a single photon," *Phys. Rev. A* **97**(3), 033807 (2018).

⁶⁸F. W. Strauch, K. Jacobs, and R. W. Simmonds, "Arbitrary control of entanglement between two superconducting resonators," *Phys. Rev. Lett.* **105**(5), 050501 (2010).

⁶⁹C. P. Yang, Q. P. Su, and S. Han, "Generation of Greenberger-Horne-Zeilinger entangled states of photons in multiple cavities via a superconducting qutrit or an atom through resonant interaction," *Phys. Rev. A* **86**(2), 022329 (2012).

⁷⁰P. B. Li, S. Y. Gao, and F. L. Li, "Engineering two-mode entangled states between two superconducting resonators by dissipation," *Phys. Rev. A* **86**(1), 012318 (2012).

⁷¹C. P. Yang, Q. P. Su, S. B. Zheng, and S. Han, "Generating entanglement between microwave photons and qubits in multiple cavities coupled by a superconducting qutrit," *Phys. Rev. A* **87**(2), 022320 (2013).

⁷²S. T. Merkel and F. K. Wilhelm, "Generation and detection of NOON states in superconducting circuits," *New J. Phys.* **12**(9), 093036 (2010).

⁷³Y. J. Zhao, C. Q. Wang, X. Zhu, and Y. X. Liu, "Engineering entangled microwave photon states via multiphoton transitions between two cavities and a superconducting qubit," *Sci. Rep.* **6**(1), 23646 (2016).

⁷⁴S. J. Xiong, Z. Sun, J. M. Liu, T. Liu, and C. P. Yang, "Efficient scheme for generation of photonic NOON states in circuit QED," *Opt. Lett.* **40**(10), 2221 (2015).

⁷⁵H. Wang, M. Mariantoni, R. C. Bialczak, M. Lenander, E. Lucero, M. Neeley, A. D. O'Connell, D. Sank, M. Weides, J. Wenner *et al.*, "Deterministic entanglement of photons in two superconducting microwave resonators," *Phys. Rev. Lett.* **106**(6), 060401 (2011).

⁷⁶Q. Zhang, W. Feng, W. Xiong, Q. P. Su, and C. P. Yang, "Generation of long-lived W states via reservoir engineering in dissipatively coupled systems," *Phys. Rev. A* **107**(1), 012410 (2023).

⁷⁷C. P. Yang, J. H. Ni, L. Bin, Y. Zhang, Y. Yu, and Q. P. Su, "Preparation of maximally-entangled states with multiple cat-state qutrits in circuit QED," *Front. Phys.* **19**(3), 31201 (2024).

⁷⁸Q. P. Su, L. Bin, Y. Zhang, M. Y. Ma, and C. P. Yang, "Generation of a hybrid W entangled state of three photonic qubits with different encodings," *Quantum Inf. Process.* **23**(1), 16 (2024).

⁷⁹C. Wang, Y. Y. Gao, P. Reinhold, R. W. Heeres, N. Ofek, K. Chou, C. Axline, M. Reagor, J. Blumoff, K. M. Sliwa *et al.*, "A Schrödinger cat living in two boxes," *Science* **352**(6289), 1087 (2016).

⁸⁰S. R. Miry, M. J. Faghihi, and H. Mahmoudi, "Nonclassicality of entangled Schrödinger cat states associated to generalized displaced Fock states," *Phys. Scr.* **98**(12), 125109 (2023).

⁸¹M. Piccolini, V. Giovannetti, and R. L. Franco, "Asymptotically deterministic robust preparation of maximally entangled bosonic states," *Phys. Rev. Res.* **6**(1), 013073 (2024).

⁸²X. Y. Yu, P. Y. Zhu, Y. Wang, M. M. Yu, C. Wu, S. C. Xue, Q. L. Zheng, Y. G. Liu, J. J. Wu, and P. Xu, "Heralded path-entangled NOON states generation from a reconfigurable photonic chip," *Chin. Phys. B* **31**(6), 064203 (2022).

⁸³Z. M. McIntyre and W. A. Coish, "Flying-cat parity checks for quantum error correction," *Phys. Rev. Res.* **6**, 023247 (2024).

⁸⁴S. Direkci, K. Winkler, C. Gut, K. Hammerer, M. Aspelmeyer, and Y. Chen, "Macroscopic quantum entanglement between an optomechanical cavity and a continuous field in presence of non-Markovian noise," *Phys. Rev. Res.* **6**, 013175 (2024).

⁸⁵T. Liu, B. Q. Guo, Y. H. Zhou, J. L. Zhao, Y. L. Fang, Q. C. Wu, and C. P. Yang, "Transfer of quantum entangled states between superconducting qubits and microwave field qubits," *Front. Phys.* **17**, 61502 (2022).

⁸⁶Q. P. Su, H. Y. Zhang, and C. P. Yang, "Transferring quantum entangled states between multiple single-photon-state qubits and coherent-state qubits in circuit QED," *Front. Phys.* **16**(6), 61501 (2021).

⁸⁷M. Mariantoni, H. Wang, R. C. Bialczak, M. Lenander, E. Lucero, M. Neeley, A. D. O'Connell, D. Sank, M. Weides, J. Wenner *et al.*, "Photon shell game in three-resonator circuit quantum electrodynamics," *Nat. Phys.* **7**(4), 287 (2011).

⁸⁸D. F. V. James and J. Jerke, "Effective Hamiltonian theory and its applications in quantum information," *Can. J. Phys.* **85**(6), 625 (2007).

⁸⁹J. Q. You, X. Hu, S. Ashhab, and F. Nori, "Low-decoherence flux qubit," *Phys. Rev. B* **75**(14), 140515(R) (2007).

⁹⁰M. Steffen, S. Kumar, D. P. DiVincenzo, J. R. Rozen, G. A. Keefe, M. B. Rothwell, and M. B. Ketchen, "High-coherence hybrid superconducting qubit," *Phys. Rev. Lett.* **105**(10), 100502 (2010).

⁹¹M. Baur, S. Filipp, R. Bianchetti, J. M. Fink, M. G. Goppl, L. Steffen, P. J. Leek, A. Blais, and A. Wallraff, "Measurement of Autler-Townes and Mollow transitions in a strongly driven superconducting qubit," *Phys. Rev. Lett.* **102**(24), 243602 (2009).

⁹²F. Yoshihara, Y. Nakamura, F. Yan, S. Gustavsson, J. Bylander, W. D. Oliver, and J. S. Tsai, "Flux qubit noise spectroscopy using Rabi oscillations under strong driving conditions," *Phys. Rev. B* **89**(2), 020503 (2014).

⁹³L. V. Abdurakhimov, I. Mahboob, H. Toida, K. Kakuyanagi, and S. Saito, "A long-lived capacitively shunted flux qubit embedded in a 3D cavity," *Appl. Phys. Lett.* **115**(26), 262601 (2019).